11-24-2011

Planning Combinatorial Disulfide Cross-Links for Protein Fold Determination

Fei Xiong
Dartmouth College

Alan M Friedman
Purdue University

Chris Bailey-Kellogg
Dartmouth College

Published in final edited form as:
J Neurosci Methods. 2012 February 15; 204(1): 111–117. doi:10.1016/j.jneumeth.2011.10.026.

Repeated assessment of orthotopic glioma pO_2 by multi-site EPR oximetry: A technique with the potential to guide therapeutic optimization by repeated measurements of oxygen

Nadeem Khan[1,3,*], **Sriram Mupparaju**[1,3], **Huagang Hou**[1,3], **Benjamin B. Williams**[1,2,3], and **Harold Swartz**[1,3]

[1]EPR Center for the Study of Viable Systems, Dartmouth Medical School, Hanover, NH 03755

[2]Section of Radiation Oncology, Dartmouth-Hitchcock Medical Center, Lebanon, NH 03756

[3]Norris Cotton Cancer Center, Dartmouth-Hitchcock Medical Center, Lebanon, NH 03756

Abstract

Tumor hypoxia plays a vital role in therapeutic resistance. Consequently, measurements of tumor pO_2 could be used to optimize the outcome of oxygen-dependent therapies, such as, chemoradiation. However, the potential optimizations are restricted by the lack of methods to repeatedly and quantitatively assess tumor pO_2 during therapies, particularly in gliomas. We describe the procedures for repeated measurements of orthotopic glioma pO_2 by multi-site electron paramagnetic resonance (EPR) oximetry. This oximetry approach provides simultaneous measurements of pO_2 at more than one site in the glioma and contralateral cerebral tissue.

The pO_2 of intracerebral 9L, C6, F98 and U251 tumors, as well as contralateral brain, were measured repeatedly for five consecutive days. The 9L glioma was well oxygenated with pO_2 of 27 - 36 mm Hg, while C6, F98 and U251 glioma were hypoxic with pO_2 of 7 - 12 mm Hg. The potential of multi-site EPR oximetry to assess temporal changes in tissue pO_2 was investigated in rats breathing 100% O_2. A significant increase in F98 tumor and contralateral brain pO_2 was observed on day 1 and day 2, however, glioma oxygenation declined on subsequent days.

In conclusion, EPR oximetry provides the capability to repeatedly assess temporal changes in orthotopic glioma pO_2. This information could be used to test and optimize the methods being developed to modulate tumor hypoxia. Furthermore, EPR oximetry could be potentially used to enhance the outcome of chemoradiation by scheduling treatments at times of increase in glioma pO_2.

Keywords

Glioma; pO_2; electron paramagnetic resonance (EPR) Oximetry; 9L; C6; F98; U251

[*]**Corresponding author**: Nadeem Khan, Ph.D., EPR Center for Viable Systems, 703 Vail, Dartmouth Medical School, Hanover, NH 03755, USA, Lab: (603) 653-3591, Fax: (603) 650-1717, Nadeem.khan@dartmouth.edu.

1. Introduction

The imbalance between oxygen supply and demand along with tumor growth and atypical angiogenesis, often leads to the development of hypoxia (pO_2; partial pressure of oxygen < 10 – 15 mmHg) in solid tumors. Subsequently, tumor hypoxia compromises treatment outcomes by facilitating DNA repair after radiation and chemotherapies. Hypoxia also leads to an alteration of gene expression, tumor progression, and metastases (Jensen, 2009; Oliver et al., 2009). In gliomas, the hypoxia responsive elements, such as Hypoxia Inducible Factor (HIF), are up-regulated and positively correlate with aggression and invasion (Jensen, 2009; Oliver et al., 2009). Consequently, tumor hypoxia has become a critical factor that must be addressed to optimize therapeutic outcome. Additionally, the dynamics of tumor pO_2 during the course of treatment is characteristic of the tumor microenvironment and proliferation. Therefore, tumor pO_2, if repeatedly measured, could be potentially used to follow efficacy, and identify responders early on during the treatments. This also will enable clinicians to prescribe alternate therapeutic interventions for non-responders.

Given the significance of hypoxia in tumor growth and response to therapies, considerable research has been carried out to develop methods for measurements of tumor oxygen, but the ability to make repeated measurements of tumor pO_2 has been challenging. Both invasive and non-invasive methods have been used to measure pO_2 in tumors, some via direct measurements of tumor pO_2 and several using parameters that relate to tumor oxygen. Each of these methods has certain benefits and limitations that will make them useful in certain settings but not appropriate for others. The polarographic (Eppendorf) and luminescence-based (OxyLite) methods do measure pO_2 directly in the tumor, but require a physical insertion of the probe in the tumor for pO_2 measurements. These can be used to obtain spatial information by making several tracks through the tumor. This invasive procedure makes these techniques unsuitable for repeated measurements of tumor pO_2 due to the trauma associated with their use. Also, measurements with Oxylite usually require a 15 - 30 min wait before the pO_2 readings are stabilized. Furthermore, the probes are somewhat fragile and very sensitive to minor movements (Brurberg et al., 2003). Methods based on nuclear magnetic resonance (NMR) have the advantage of widely available instrumentation. Blood oxygen level dependent (BOLD) imaging (Baudelet and Gallez, 2002) is widely available, including clinically, but provides only the relative amount of deoxyhemoglobin in the blood in the volume measured, which cannot be directly related to tissue oxygen in the tumor. Using more specialized equipments, ^{19}F-NMR spectroscopy (Hunjan et al., 2001), and Overhauser methods (Krishna et al., 2002) have the potential to provide direct measurements of tumor oxygen but require the injection of the probe, and these injections need to be done each time for repeated measurements.

We have focused on the development of EPR oximetry using particulates for the assessment of absolute pO_2 in the tumors. The basis of EPR oximetry is the paramagnetic nature of molecular oxygen, which therefore affects the EPR spectra of other paramagnetic species in its vicinity by altering their relaxation rates. The magnitude of the effects is directly related to the amount of oxygen that is present in the environment of the paramagnetic materials such as LiPc (lithium phthalocyanine) crystals. EPR oximetry using particulates requires one time implantation of the oximetry probe using a minimally invasive method, but all further procedures for pO_2 measurement are entirely non-invasive and can be repeated as often as desired. A temporal resolution of the order of several seconds, and oxygen sensitivity of 1 mm Hg could be achieved using lithium phathalocyanine (LiPc) in vivo. With RF fields at 1200 MHz and surface-loop resonators, pO_2 measurements can be made within tissues as deep as 10 mm from the surface; however implantable resonators are being developed to enable pO_2 measurements at much greater depths with excellent signal to noise ratio (Hou et al., 2011; Li et al., 2010). In order to asses oxygen heterogeneity, a spatial resolution of up

to 1 mm are achievable using multiple implants of oxygen sensitive particulates, and by applying a magnetic field gradients to differentiate the independent signals from each implant (Khan et al., 2009; Khan et al., 2010). We describe the procedure for the oximetry of orthotopic gliomas using LiPc implants by EPR. The feasibility of this method is demonstrated by repeated assessments of experimental 9L, C6, F98 and human xenograft U251 glioma and contralateral brain pO_2 simultaneously by multi-site EPR oximetry. We also report the effect of 100% O_2 breathing on the F98 glioma and contralateral brain pO_2 in experiments repeated for five consecutive days. This oximetry approach could also be used to study the effect of other neuropathology, such as, the consequence of ischemia-reperfusion injury on the intracerebral tissue pO_2 and develop methods to minimize the tissue damage by investigating treatment protocols that can improve the oxygen levels in the affected areas of the brain (Hou et al., 2007; Hou et al., 2005; Williams et al., 2007). EPR imaging using water soluble probes can be used to obtain 3D oxygen maps of tumors with temporal resolution of approximately 10 min, oxygen sensitivity of 1 mm Hg, and spatial resolution of 1.5 mm, with repeated injection of probes required for each measurement (Epel et al., 2011).

2. Materials and Methods

2.1 Animals and Tumor models

All animal procedures were conducted in strict accordance with the National Institutes of Health Guide for the Care and Use of Laboratory Animals and were approved by the Institutional Animal Care and Use Committee of Dartmouth Medical School. The experimental 9L gliomas have sarcomatous appearances histologically, while the C6 are classified as astrocytomas and have gene expressions similar to that of human gliomas (Barth and Kaur, 2009). However, both 9L and C6 are immunogenic, and therefore, caution should be exercised in analyzing therapeutic effects. F98 is an anaplastic glioma with minor sarcomatous characteristics (Barth and Kaur, 2009). The F98 glioma is weakly immunogenic with growth and invasive characteristics consistent with human glioblastomas. The U251 xenograft glioma is an astrocytic phenotype with histological features similar to those of the human glioblastoma, including angiogenesis, and tumor cell infiltration (Candolfi et al., 2007). Fischer and Wistar rats (200 - 250g), which are syngeneic hosts for 9L/F98 and C6 gliomas respectively, were purchased from Charles River Laboratory (MA) and housed in the animal resource facility at Dartmouth Medical School. The athymic nu/nu (homozygous, 15 - 20 g) mice were purchased from Charles River Laboratory (MA) and housed in the quarantine quarters of the animal resource facility at Dartmouth Medical School.

2.2 Glioma cells culture and intracerebral tumor inoculation

The 9L, C6, and F98 cells were purchased from ATCC (Manassas, VA) and propagated in Dulbecco's Modified Eagle's Medium with 4.5 g/L glucose, 1 mM sodium pyruvate, 10% FBS and 1% penicillin-streptomycin. For tumor inoculation, the cells were detached from the culture flask by trypsinization (0.25% trypsin, Mediatech Inc, Manassas, VA), and washed three times with the medium without serum or additives. The cell numbers were determined by Countess automated cell counter (Invitrogen, CA) and a suspension of 50,000 cells/10 μl was prepared for injection in rat brain.

The rats were anesthetized using 2.5% isoflurane with 30% oxygen through a nose cone, and the head was immobilized on a stereotaxic apparatus (ASI Instruments, MI), Figure 1. The head was shaved and aseptically prepared with Betadine and 70% ethanol. Each rat was inoculated with one tumor in the left hemisphere by slow injection of the cells over 2 min with a 25-gauge needle through a burr hole at 3 mm behind bregma (anteroposterior, – 3.0

mm), 1.5 mm from midline (mediolateral, 1.5 mm) and at 3.5 mm depth from the skull (dorsoventral, 3.5 mm). After injection of the tumor cells, the burr hole was cleaned and sealed with bone wax, and the skin was sutured.

The U251 cells were obtained from NCI and cultured in RPMI 1640 medium using the procedure described above. The U251 tumors were established by slow injection of 1×10^6 cells/10 μl over 5 min with a 25-gauge needle through a burr hole at the following coordinates: anteroposterior, −1.7 mm; mediolateral, 1.5 mm; and dorsoventral, 2.0 mm in the left hemisphere. After injection of the tumor cells, the burr hole was cleaned and sealed with bone wax, and the skin was sutured.

2.3 Implantation of oxygen sensitive particulate probe

The paramagnetic LiPc crystals are synthesized in our laboratory by an electrochemical method and their physicochemical properties have been described previously (Liu et al., 1993). After implantation, the LiPc deposits remain in the interstitial compartment of the tumor with minimal evidence of edema or infiltration of inflammatory cells. A minor accumulation of red blood cells and some necrotic cells around the LiPc deposits is typically observed, which perhaps reflect the normal histological pattern of the tumor. In order to enhance the biocompatibility, in particularly for clinical applications, various encapsulations of the oximetry probes in biocompatible and inert polymers have been developed, which could be potentially retrieved after the treatments (Dinguizli et al., 2006; Meenakshisundaram et al., 2009a; Meenakshisundaram et al., 2009b).

The LiPc crystals are metabolically inert and have a single sharp EPR line. Because oxygen is also paramagnetic, the presence of oxygen near LiPc alters the EPR signal in proportion to the partial pressure of oxygen in the tissue. By using an appropriate calibration, the width of the EPR absorption peak of the LiPc crystals provides a sensitive measurement of tissue pO_2. The EPR spectra reflect the average pO_2 on the surface of the crystals. The high density of the unpaired spins combined with a narrow intrinsic line width of LiPc makes it a suitable probe for the measurements of tissue pO_2 with EPR (Liu et al., 1993). For LiPc implantation, the rats were anesthetized (2.5% isoflurane, 30% O_2) and the skin was re-incised at the midline after 7 days of cell injection. Two aggregates of LiPc crystals (40 - 60 μg/each) were loaded in 25-gauge needle/plungers and injected at anteroposterior, – 3.0 mm, and mediolateral, 1.5 mm and 3.5 mm in the left hemisphere at a depth of 2 mm from the skull surface. One aggregate of LiPc crystals was injected at the same depth in the right hemisphere at mediolateral, 1.5 mm and anteroposterior, 3.0 mm. Due to relatively small size of the mouse brain as compared to the rats, only one aggregate of LiPc was injected in the U251 glioma using the same bur hole used for cell injections at a depth of 2 mm from the skull surface. One aggregate of LiPc was also injected at the same depth in the right hemisphere at anteroposterior, −1.7 mm and mediolateral, 1.5 mm to assess contralateral brain pO_2. These injections created LiPc deposits with a surface area of approximately 0.5 - 1.5 mm^2, therefore, these deposits samples a large enough region that includes several capillaries and thus provides an average intracerebral tumor and contralateral brain pO_2 simultaneously by multi-site EPR oximetry described below. The median survival of the animals was approximately 25 – 28 days after cell injections. This survival time is ideal for therapeutic study as it allows an adequate time to treat the tumors and follow the outcome.

2.4 High-Spatial Resolution Multi-Site (HSR-MS) EPR Oximetry

A lack of an appropriate oximetry method for repeated assessment of intracerebral pO_2 has restricted the use of orthotopic gliomas to assess the effect of interventions designed to manipulate hypoxia for the optimization of chemoradiation. The use of ectopic tumors,

instead, is likely to influence the results due to tissue specific effects on tumor microenvironment.

The basic principles of EPR oximetry have been described earlier (Ahmad and Kuppusamy, 2010; Hyodo et al., 2010; Swartz and Clarkson, 1998). HSR-MS EPR oximetry provides pO_2 measurements using multiple LiPc implants in the brain (Khan et al., 2009; Khan et al., 2010; Khan et al., 2007; Williams et al., 2007). This technique uses two spectra that are acquired with magnetic field gradients of different magnitudes and estimates the pO_2 at each implant site via an analytic relationship between the absorption line widths of the spectra. This technique has been used to simultaneously assess pO_2 within areas of pathophysiology and a control site (Khan et al., 2009; Khan et al., 2010; Khan et al., 2007; Williams et al., 2007). The HSR-MS method has spatial resolution of 1 mm, which allows us to place two LiPc implants in a tumor with a length of ~ 4 mm. The principle of multi-site oximetry using magnetic field gradients have been described earlier (Grinberg et al., 2001; Williams et al., 2007). More LiPc implants can be used to increase the spatial information, if desired. Additionally, implantable resonators with 3 - 4 probes are being developed to simultaneous assess tissue pO_2 at multiple locations in the tumors and contralateral brain of rodents with good signal to noise ratio (Li et al., 2010).

For pO_2 measurements, the animals were anesthetized (1.5% isoflurane, 30% O_2) and positioned between the poles of the 400 Gauss EPR magnets. An external loop resonator with resonant frequency of ~1200 MHz was gently placed on the head over the implantation sites. For data acquisition, two EPR scans with magnetic field gradients of 0.28 G/cm and 0.56 G/cm and modulation amplitudes of 0.16 G and 0.32 G respectively were acquired. The scan widths were scaled in proportion to the gradient magnitudes and were 5.6 G and 10.9 G, respectively. Similarly, the scan times were 30 sec and 60 sec respectively for low and high gradient EPR scans. The magnitude of the gradient required to separate the spectra, while minimizing any broadening of the EPR lines, depends on the actual line width and size of the implants and distance between them. Experimental conditions, field gradient and limitations of the multi-site EPR oximetry were discussed by Smirnov et al. (Smirnov et al., 1993). The line width of the EPR signal was converted to pO_2 using the calibration of the batch of LiPc used in this study, Figure 2. We have extensive calibration data, which indicates no significant change in the calibration after the implants are removed from the tissue. No significant differences in the pO_2 recorded from the two LiPc implants in each tumor was observed; therefore these were pooled to obtain an average tumor pO_2. The body temperature of the animals during pO_2 measurements was monitored using a rectal probe and maintained at 37 ± 0.5°C by keeping the body warm with a warm air blower and water pad. In order to assess the potential of HSR-MS EPR oximetry for the measurements of temporal changes in tissue pO_2, the anesthetized rats with F98 glioma were allowed to breath 30% O_2 for 25 - 30 min (baseline) and then the inhaled gas was switched to 100% O_2 and EPR measurements were continued for another 60 min. These experiments were repeated for five consecutive days to assess the effect of repeated hyperoxia on glioma oxygenation. The EPR spectra were recorded at 4 mW to avoid power saturation, with scan times varying from 30 - 60 seconds. The spectra were averaged for 5 min each to enhance the signal to noise ratio for precise pO_2 measurements. The EPR spectra were acquired using LabVIEW acquisition routine and analyzed using software written in Matlab for spectral fitting, Figure 5A.

2.5 Magnetic Resonance Imaging (MRI)

The growth of the intracerebral tumors and the location of LiPc were confirmed on day 0 (24 hr prior to the experiment) from T_1-weighted images acquired after the intraperitoneal injection of 0.2 mmol/kg of gadopentate (Magnevist, Bayer Healthcare). The images were acquired on a 7T horizontal animal magnet with a bore of 20 cm (Magnex Scientific Ltd,

U.K) equipped with actively shielded imaging gradients, maximum gradient strength 77 G/cm, clear bore 90 mm (Resonance Research Incorporated Ltd, MA), and interfaced to a Varian Inova Unity console (Varian Inc, CA). A multi-slice spin echo sequence was used to acquire T_1-weighted images for tumor volume determination 5 min after gadopentate injection with the acquisition parameters: TR = 700 ms, TE 8 ms, 20 slices, no slice gap, slice thickness 1 mm, Field of View (FOV) = 30 mm, 128 × 128, 2 signal averages per phase encoding step. The tumor volumes were calculated by drawing region of interest on the contrast enhanced tumor regions using Varian in-built BROWSER software and were approximately 60 – 100 mm^3 in these experiments.

2.6 Statistical analysis

A paired t-test was used to account for animal heterogeneity in comparison of pO_2 over days and an unpaired t-test was used to determine the statistical significance between groups. All data are expressed as Mean ± SEM; n is the number of animals in each group.

3. Results

3.1 Intracerebral tumor and contralateral brain pO_2 by HSR-MS EPR oximetry

The intracerebral tumors and contralateral brain pO_2 measured simultaneously using HSR-MS oximetry are summarized in Figures 3 and 4. The pO_2 of 9L glioma on day 1 (day 14 after cell injection) was 37 ± 7 mmHg, however, the C6, F98 and U251 glioma were significantly hypoxic with a pO_2 of 10 ± 2, 8 ± 0.7 and 9.1 ± 1.4 mmHg respectively, Figure 3. No significant change in the 9L, C6 and U251 glioma pO_2 was observed in measurements repeated for five consecutive days. On the other hand, a significant decrease in F98 glioma pO_2 (only on day 4 as compared to day 1) was observed.

The contralateral brain pO_2 of the rats bearing 9L, C6 and F98 gliomas in the left hemisphere was 35 ± 4, 42 ± 3, and 38 ± 7 mm Hg respectively, Figure 4. Interestingly, the contralateral brain pO_2 of the mice was 68 ± 6 mm Hg and was significantly higher than the contralateral brain pO_2 of the rats. The contralateral brain pO_2 of the rats as well as the mice bearing each glioma type did not change significantly in the measurements repeated for five consecutive days.

3.2 Effect of 100% O_2 breathing on intracerebral F98 tumor and contralateral brain pO_2

The effect of 100% O_2 breathing on the pO_2 of intracerebral F98 and contralateral brain pO_2 is summarized in Figures 5 and 6. Typical EPR spectra obtained from rats breathing 30% O_2 are shown in Figure 5A. In this rat, the contralateral brain pO_2 was 33 mmHg, while the pO_2 of the F98 glioma was 15 and 13 mmHg. A significant increase in the contralateral brain and F98 glioma pO_2 was observed when the breathing gas was switched from 30% O_2 to 100% O_2, Figure 5B.

The temporal changes in the pO_2 of F98 glioma and contralateral brain in the experiments repeated for five consecutive days are summarized in Figures 6 and 7. The mean tumor pO_2 on day 1 was 14.2 ± 2 mm Hg, which significantly declined to 8 ± 0.9 and 8.4 ± 1 mmHg on days 4 and 5 respectively. The breathing of 100% O_2 resulted in a significant increase in the tumor pO_2 on day 1. Similar results were obtained in experiments repeated on day 2; however the response to 100% O_2 breathing significantly declined on subsequent days.

The mean contralateral brain pO_2 of the rats breathing 30% O_2 was 44 ± 5 mm Hg on day 1 and no significant difference was observed in experiments repeated on subsequent days. A significant increase in pO_2 was evident during 100% O_2 breathing on day 1, however, the

pO_2 varied during measurements for 60 min. Similar results were obtained on days 2 - 4, while no significant increase in pO_2 occurred on day 5.

4. Discussion

The oximetry methods that can provide direct assessments of tumor pO_2, which can be repeated as desired, will be especially useful to test the efficacy of interventions being developed to modulate tumor hypoxia for therapeutic benefits. HSR-MS EPR oximetry using particulates allows repeated assessments of tumor pO_2 during the entire course of therapeutic interventions. The placement of the paramagnetic material is minimally invasive (it usually requires an insertion via a 23 - 25 gauge needle), but all subsequent procedures for pO_2 measurements are entirely non-invasive.

Our results indicate that the orthotopic C6, F98 and U251 gliomas are hypoxic, whereas 9L gliomas are well oxygenated. To the best of our knowledge, this is the first report of repeated assessment of orthotopic U251 glioma pO_2 over days. No significant change in the pO_2 of 9L, C6 and U251 glioma was observed on repeated measurements for 5 consecutive days. However, the pO_2 of F98 glioma significantly declined on day 4 as compared to day 1. No significant difference in the contralateral brain pO_2 of rats bearing 9L, C6 and F98 gliomas was observed. However, the contralateral brain pO_2 of the mice were significantly higher than the rats; this warrants further investigation. The pO_2 of the experimental tumors and contralateral brain in the rats are similar to our earlier findings (Khan et al., 2009; Khan et al., 2010). The temporal changes in the F98 glioma pO_2 during 100% O_2 breathing varied over time and a significant decline in oxygenation was evident in experiments repeated on subsequent days. A similar effect of 100% O_2 inhalation on the pO_2 of contralateral brain was observed. These results indicate a day to day variation in the response of the gliomas to 100% O_2 breathing, which highlights the need of repeated assessments of glioma pO_2 during interventions designed to modulate tumor hypoxia. The temporal information of the glioma pO_2 during hyperoxic interventions is crucial to synergize these approaches with radiotherapy by scheduling radiations at times of increase in glioma pO_2 to enhance therapeutic outcome.

Using this multi-site oximetry approach with particulate probes, the region covered by EPR oximetry is representative of the tumor since it spans the intercapillary distance of normal and tumor tissue. Normal rat brain is reported to have an inter-capillary distance of about 45 μm (Lierse, 1963) and a capillary density of 150 - 300 per mm^2 (Cavaglia et al., 2001). Therefore, multi-site EPR oximetry is sampling a region that includes, at minimum, scores of capillaries and potentially a region that spans the heterogeneous tumor structure. A major advantage of EPR oximetry is that it provides a means to get repeated measurements of tumor pO_2. As a tumor grows or necroses, it is possible that the location of the particle within the tumor could change or the microenvironment of the tumor around it can be altered. This potential drawback can be overcome by determining the structure and functional status of the tissue around the material as the experiment progresses by using the methods such as PET and CT. Additionally, oximetry at multiple sites will make it feasible to determine if there are localized anomalies.

In summary, HSR-MS EPR oximetry offers several advantages over other methods: (i) it provides a direct measurement of intracerebral tumor pO_2 (as compared to indirect techniques such as BOLD NMR); (ii) measurements provide quantitative pO_2 data (as compared to techniques such as misonidazole, which provide information on the occurrence of hypoxia but usually do not provide quantitative information on the pO_2); (iii) pO_2 measurements can be made continuously and repeatedly as desired; (iv) oxygen-sensitive materials used in EPR oximetry are metabolically inert; and (v) placement of the

paramagnetic material is minimally invasive and all subsequent measurements are entirely non-invasive. The advantages and limitations of the various oximetry approaches have been reviewed earlier (Evans et al., 2011; Springett and Swartz, 2007; Swartz et al., 1997; Swartz and Dunn, 2003). EPR oximetry using single implants of oxygen sensitive India ink is currently being tested for pO_2 measurements in patients with tumors at depths of less than 10 mm from the surface (Khan et al., 2007; Swartz et al., 2004; Williams et al., 2010). Implantable resonators are being developed, which will allow oximetry at depths of up to 100 mm from the surface (Hou et al., 2011; Li et al., 2010). We are currently investigating the feasibility of intracerebral tissue pO_2 measurements at depths of 30 mm in large subjects with the goal to extend its application in the clinics. The implantable resonators have an added advantage of significantly higher signal to noise ratio as compared to LiPc deposits. Studies are ongoing to test the feasibility of oximetry with multiple-loop implantable resonators to investigate pO_2 at several locations in the intracerebral human xenograft tumors along with measurements of the contralateral brain in mice.

Acknowledgments

This work was supported by NIH grant CA120919, and Prouty Pilot Project Award from the Friends, Norris Cotton Cancer Center to NK and used the facilities of the EPR Center.

6. References

Ahmad R, Kuppusamy P. Theory, instrumentation, and applications of electron paramagnetic resonance oximetry. Chem Rev. 2010; 110:3212–36. [PubMed: 20218670]

Barth RF, Kaur B. Rat brain tumor models in experimental neuro-oncology: the C6, 9L, T9, RG2, F98, BT4C, RT-2 and CNS-1 gliomas. J Neurooncol. 2009; 94:299–312. [PubMed: 19381449]

Baudelet C, Gallez B. How does blood oxygen level dependent (BOLD) contrast correlate with the oxygen partial pressure (pO_2) inside tumors? Mag. Res. Med. 2002; 48:980–6.

Brurberg KG, Graff BA, Rofstad EK. Temporal heterogeneity in oxygen tension in human melanoma xenografts. British Journal of Cancer. 2003; 89:350–6. [PubMed: 12865929]

Candolfi M, Curtin JF, Nichols WS, Muhammad AG, King GD, Pluhar GE, McNiel EA, Ohlfest JR, Freese AB, Moore PF, Lerner J, Lowenstein PR, Castro MG. Intracranial glioblastoma models in preclinical neuro-oncology: neuropathological characterization and tumor progression. J Neurooncol. 2007; 85:133–48. [PubMed: 17874037]

Cavaglia M, Dombrowski SM, Drazba J, Vasanji A, Bokesch PM, Janigro D. Regional variation in brain capillary density and vascular response to ischemia. Brain Research. 2001; 910:81–93. [PubMed: 11489257]

Dinguizli M, Jeumont S, Beghein N, He J, Walczak T, Lesniewski PN, Hou H, Grinberg OY, Sucheta A, Swartz HM, Gallez B. Development and evaluation of biocompatible films of polytetrafluoroethylene polymers holding lithium phthalocyanine crystals for their use in EPR oximetry. Biosens Bioelectron. 2006; 21:1015–22. [PubMed: 16368480]

Epel B, Sundramoorthy SV, Barth ED, Mailer C, Halpern HJ. Comparison of 250 MHz electron spin echo and continuous wave oxygen EPR imaging methods for in vivo applications. Med Phys. 2011; 38:2045–52. [PubMed: 21626937]

Evans CE, Mattock K, Humphries J, Saha P, Ahmad A, Waltham M, Patel A, Modarai B, Porter L, Premaratne S, Smith A. Techniques of assessing hypoxia at the bench and bedside. Angiogenesis. 2011

Grinberg OY, Smirnov AI, Swartz HM. High spatial resolution multi-site EPR oximetry: the use of a convolution-based fitting method. J. Magn. Reson. 2001; 152:247–58. [PubMed: 11567578]

Hou H, Grinberg O, Williams B, Grinberg S, Yu H, Alvarenga DL, Wallach H, Buckey J, Swartz HM. The effect of oxygen therapy on brain damage and cerebral pO(2) in transient focal cerebral ischemia in the rat. Physiological measurement. 2007; 28:963–76. [PubMed: 17664686]

Hou H, Grinberg OY, Grinberg SA, Demidenko E, Swartz HM. Cerebral tissue oxygenation in reversible focal ischemia in rats: multi-site EPR oximetry measurements. Physiological measurement. 2005; 26:131–41. [PubMed: 15742885]

Hou H, Li H, Dong R, Mupparaju S, Khan N, Swartz H. Cerebral oxygenation of the cortex and striatum following normobaric hyperoxia and mild hypoxia in rats by EPR oximetry using multi-probe implantable resonators. Advances in experimental medicine and biology. 2011; 701:61–7. [PubMed: 21445770]

Hunjan S, Zhao D, Constantinescu A, Hah nE, Antich P, Mason R. Tumor oximetry: demonstration of an enhanced dynamic mapping procedure using fluorine-19 echo planar magnetic resonance imaging in the Dunning prostate R3327-AT1 rat tumor. International Journal of Radiation Oncology, Biology, Physics. 2001; 49:1097–108.

Hyodo F, Matsumoto S, Hyodo E, Matsumoto A, Matsumoto K, Krishna MC. In vivo measurement of tissue oxygen using electron paramagnetic resonance spectroscopy with oxygen-sensitive paramagnetic particle, lithium phthalocyanine. Methods in molecular biology (Clifton, N.J. 2010; 610:29–39.

Jensen RL. Brain tumor hypoxia: tumorigenesis, angiogenesis, imaging, pseudoprogression, and as a therapeutic target. J Neurooncol. 2009; 92:317–35. [PubMed: 19357959]

Khan N, Li H, Hou H, Lariviere JP, Gladstone DJ, Demidenko E, Swartz HM. Tissue pO2 of orthotopic 9L and C6 gliomas and tumor-specific response to radiotherapy and hyperoxygenation. International journal of radiation oncology, biology, physics. 2009; 73:878–85.

Khan N, Mupparaju S, Hekmatyar SK, Hou H, Lariviere JP, Demidenko E, Gladstone DJ, Kauppinen RA, Swartz HM. Effect of hyperoxygenation on tissue pO2 and its effect on radiotherapeutic efficacy of orthotopic F98 gliomas. International journal of radiation oncology, biology, physics. 2010; 78:1193–200.

Khan N, Williams BB, Hou H, Li H, Swartz HM. Repetitive tissue pO2 measurements by electron paramagnetic resonance oximetry: current status and future potential for experimental and clinical studies. Antioxidants & redox signaling. 2007; 9:1169–82. [PubMed: 17536960]

rishna MC, English S, Yamada K, Yoo J, Murugesan R, Devasahayam N, Cook JA, Golman K, Ardenkjaer-Larsen JH, Subramanian S, Mitchell JB. Overhauser enhanced magnetic resonance imaging for tumor oximetry: Coregistration of tumor anatomy and tissue oxygen concentration. PNAS. 2002; 99:2216–21. [PubMed: 11854518]

Li H, Hou H, Sucheta A, Williams BB, Lariviere JP, Khan MN, Lesniewski PN, Gallez B, Swartz HM. Implantable resonators--a technique for repeated measurement of oxygen at multiple deep sites with in vivo EPR. Advances in experimental medicine and biology. 2010; 662:265–72. [PubMed: 20204802]

Lierse W. Die Kapillardichte im Wirbeltiergehirn. Acta Anat (Basel). 1963; 54:1–31. [PubMed: 14082531]

Liu KJ, Gast P, Moussavi M, Norby SW, Vahidi N, Walczak T, Wu M, Swartz HM. Lithium phthalocyanine: a probe for electron paramagnetic resonance oximetry in viable biological systems. Proc Natl Acad Sci U S A. 1993; 90:5438–42. [PubMed: 8390665]

Meenakshisundaram G, Eteshola E, Pandian RP, Bratasz A, Lee SC, Kuppusamy P. Fabrication and physical evaluation of a polymer-encapsulated paramagnetic probe for biomedical oximetry. Biomed Microdevices. 2009a; 11:773–82. [PubMed: 19291409]

Meenakshisundaram G, Eteshola E, Pandian RP, Bratasz A, Selvendiran K, Lee SC, Krishna MC, Swartz HM, Kuppusamy P. Oxygen sensitivity and biocompatibility of an implantable paramagnetic probe for repeated measurements of tissue oxygenation. Biomed Microdevices. 2009b; 11:817–26. [PubMed: 19319683]

Oliver L, Olivier C, Marhuenda FB, Campone M, Vallette FM. Hypoxia and the malignant glioma microenvironment: regulation and implications for therapy. Curr Mol Pharmacol. 2009; 2:263–84. [PubMed: 20021464]

Smirnov AI, Norby SW, Clarkson RB, Walczak T, Swartz HM. Simultaneous multi-site EPR spectroscopy in vivo. Magn. Reson. Med. 1993; 30:213–20. [PubMed: 8396190]

Springett R, Swartz HM. Measurements of oxygen in vivo: overview and perspectives on methods to measure oxygen within cells and tissues. Antioxidants & redox signaling. 2007; 9:1295–301. [PubMed: 17576162]

Swartz HM, Clarkson RB. The measurement of oxygen in vivo using EPR techniques. Physics in medicine and biology. 1998; 43:1957–75. [PubMed: 9703059]

Swartz HM, Dunn J, Grinberg O, O'Hara J, Walczak T. What does EPR oximetry with solid particles measure--and how does this relate to other measures of PO2? Advances in experimental medicine and biology. 1997; 428:663–70. [PubMed: 9500113]

Swartz HM, Dunn JF. Measurements of oxygen in tissues: overview and perspectives on methods. Advances in experimental medicine and biology. 2003; 530:1–12. [PubMed: 14562699]

Swartz HM, Khan N, Buckey J, Comi R, Gould L, Grinberg O, Hartford A, Hopf H, Hou H, Hug E, Iwasaki A, Lesniewski P, Salikhov I, Walczak T. Clinical applications of EPR: overview and perspectives. NMR in biomedicine. 2004; 17:335–51. [PubMed: 15366033]

Williams BB, Hou H, Grinberg OY, Demidenko E, Swartz HM. High spatial resolution multisite EPR oximetry of transient focal cerebral ischemia in the rat. Antioxidants & redox signaling. 2007; 9:1691–8. [PubMed: 17678442]

Williams BB, Khan N, Zaki B, Hartford A, Ernstoff MS, Swartz HM. Clinical electron paramagnetic resonance (EPR) oximetry using India ink. Advances in experimental medicine and biology. 2010; 662:149–56. [PubMed: 20204785]

Research highlights

- EPR oximetry using particulate probes provide repeated assessment of temporal changes in orthotopic glioma pO_2; a unique capability not available with any other technique
- Simultaneous measurement of glioma and contralateral brain pO_2 by the multi-site EPR oximetry provides site specific tissue pO_2 information during treatments.
- Orthotopic 9L gliomas are well oxygenated while C6, F98 and U251 glioma are hypoxic.
- The effect of 100% O_2 inhalation on F98 glioma pO_2 declined over days, which highlights the significance of repeated oximetry for a potential optimization of the approaches developed to modulate tumor hypoxia and rationally combine with radiotherapy to enhance the outcome.

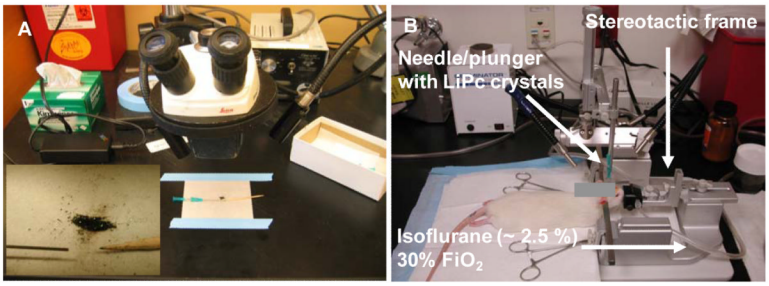

Figure 1.

(A) LiPc crystals are loaded under a microscope in 25 gauge needles (approx 40 - 60 μg) for injection in the rat brain. The insert shows the LiPc crystals, needle and a wooden plunger used to load the crystals in the needle. The bevel of the needles can be blunted to precisely control the depth of the implants and potentially reduce tissue injury. (B) The stereotaxic apparatus used to inject the cells and LiPc aggregates in the brain of rats.

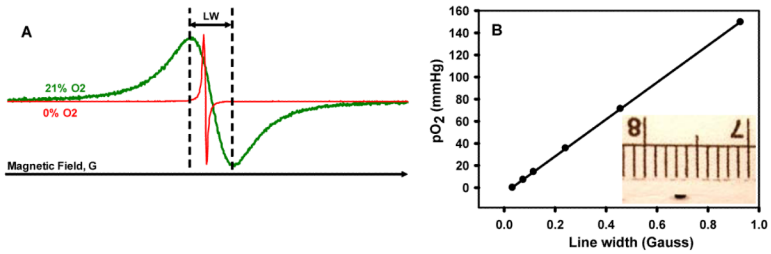

Figure 2.

(A) Typical in vitro EPR spectra of the LiPc crystals acquired at 1200 MHz during perfusion with 21% (air) and 0% O_2. (B) Change in the line width of the LiPc crystals with change in pO_2. This calibration is used to convert the line width observed in vivo to tissue pO_2. Each batch of LiPc crystals is calibrated prior to in vivo experiments. The insert shows the size of the LiPc implants (~ 1 mm) used for pO_2 measurements by EPR oximetry.

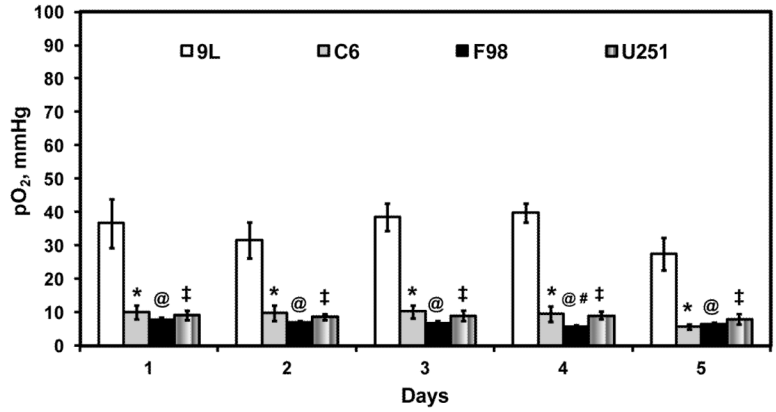

Figure 3.

Tissue pO_2 of intracerebral 9L, C6, and F98 gliomas in untreated rats. The cells were injected on day -14 and the measurements were started on day 1 for five consecutive days. Mean ± SEM, n = 5 - 6. $P < 0.05$, *9L vs C6; $^{@}$9L vs F98; ‡9L vs U251; $^{\#}$F98 day 1 vs day 4.

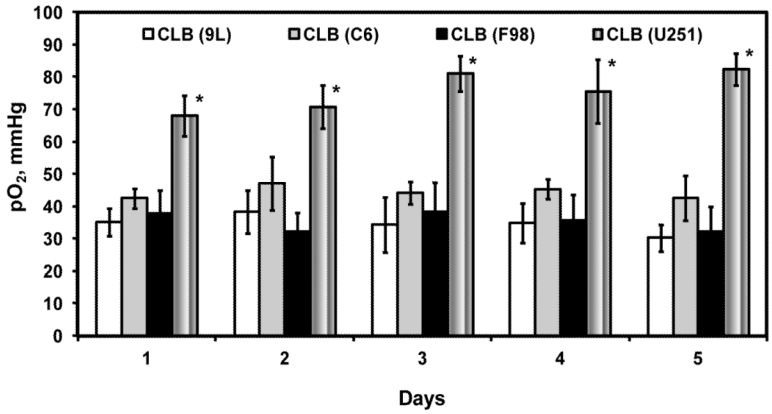

Figure 4.

Tissue pO_2 of the contralateral brain in rats inoculated with 9L, C6, and F98 gliomas on day -14. The pO_2 measurements were initiated on day 1 and repeated for four subsequent days by HSR-MS EPR oximetry. Mean ± SEM, n = 5 - 6. $P < 0.05$, *U251 vs 9L, C6, and F98.

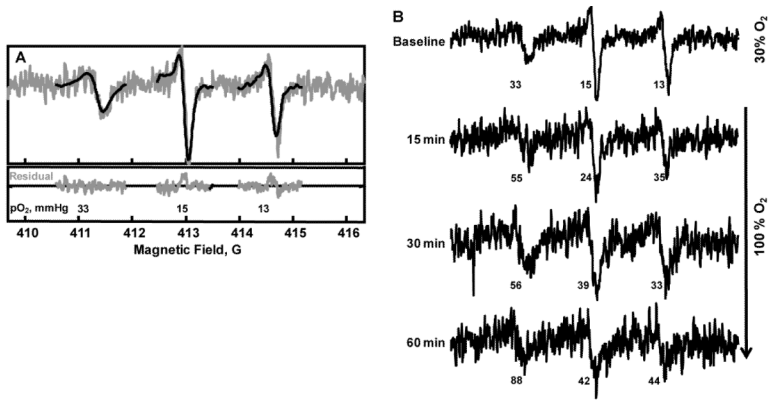

Figure 5.

Typical in vivo EPR spectra acquired by HSR-MS EPR oximetry from a rat with an intracerebral F98 tumor in the left hemisphere. (A) The EPR signal on the left was acquired from the LiPc implant in the brain (right hemisphere) and the other two signals were acquired from LiPc implants in the tumor (left-hemisphere). The pO_2 reported by the LiPc implants in the tumor were pooled to obtain average tumor pO_2. (B) Temporal changes in the pO_2 of the contralateral brain and F98 tumor in the rat breathing 30% O_2 (baseline) and after the gas was switched to 100% O_2.

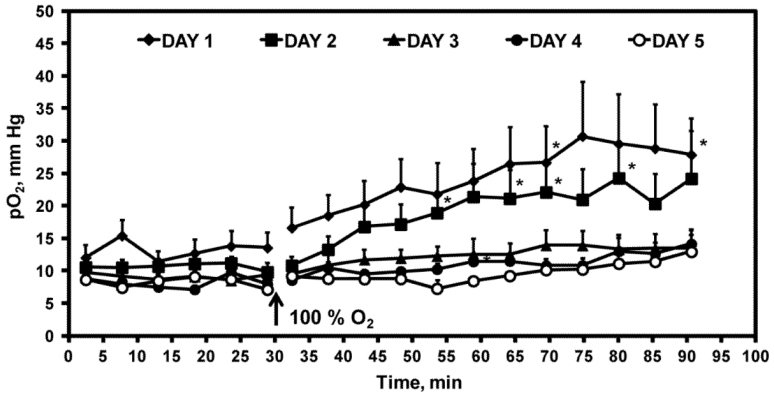

Figure 6.

Temporal changes in intracerebral F98 tumor pO_2 in rats breathing 30% O_2 (baseline) and after the inhaled gas was switched to 100% O_2. The experiment was repeated for five consecutive days. Mean ± SEM, n = 5 - 6. $P < 0.05$, *pO_2 100% O_2 vs mean baseline pO_2.

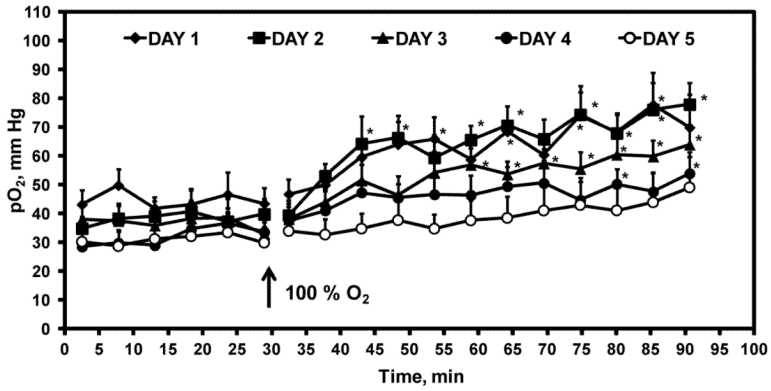

Figure 7.

Temporal changes in the contralateral brain pO_2 of rats breathing 30% O_2 (baseline) and when the inhaled gas was switched to 100% O_2. The experiment was repeated for five consecutive days. Mean ± SEM, n = 5 - 6. $P < 0.05$, *pO_2 100% O_2 vs mean baseline pO_2.